



MET-AICE v1.0: an operational data-driven sea ice prediction system for the European Arctic

Cyril Palerme¹, Johannes Röhrs², Thomas Lavergne², Jozef Rusin², Are Frode Kvanum^{1, 4},
Atle Macdonald Sørensen², Arne Melsom², Julien Brajard³, Martina Idžanović², Marina Durán Moro²,
and Malte Müller^{1, 4}

¹Development Centre for Weather Forecasting, Norwegian Meteorological Institute, Oslo, Norway

²Ocean Department, Norwegian Meteorological Institute, Oslo, Norway

³Nansen Environmental and Remote Sensing Center, Bergen, Norway

⁴Section for Meteorology and Oceanography, Department of Geosciences, University of Oslo, Oslo, Norway

Correspondence: Cyril Palerme (cyril.palerm@met.no)

Abstract. There is an increasing need for reliable short-term sea ice forecasts that can support maritime operations in polar regions. While numerous studies have shown the potential of machine learning for sea ice forecasting, there are currently only a few operational data-driven sea ice prediction systems. Here, we introduce MET-AICE, a prediction system providing sea ice concentration forecasts for the next 10 days in the European Arctic. To our knowledge, it is the first operational data-driven prediction system designed for short-term sea ice forecasting. MET-AICE has been trained to predict sea ice concentration observations from the Advanced Microwave Scanning Radiometer 2 (AMSR2) at 5 km resolution. After one year of operation, we show that MET-AICE considerably outperforms persistence of AMSR2 observations (root mean square error about 31 % lower on average) and forecasts from the Barents-2.5km physically-based model (root mean square error about 50 % lower on average).

1 Introduction

There are growing economic and geopolitical interests in the Arctic affecting various sectors such as shipping, tourism, fishing, and resource extraction (Stocker et al., 2020; Gunnarsson, 2021; Müller et al., 2023). This has resulted in a recent increase of the maritime traffic of about 7 % per year over the past decade (Müller et al., 2023). However, sea ice still remains a source of hazards, in particular due to the remoteness of the polar regions. In order to reduce the risk of accidents, seafarers going to ice infested waters are required to get sea ice information before their journeys by the International Code for Ships Operating in Polar Waters since 2017 (Polar Code; Deggin, 2018). The primary source of sea ice information used by seafarers navigating in the Arctic usually consists of sea ice charts produced by national ice services and satellite products (Wagner et al., 2020; Copeland et al., 2024). While the current conditions can be assessed using such observations (though some of these data might already be outdated in areas with fast changing conditions), they do not allow to anticipate the sea ice evolution during the next few days. For route planning, skillful sea ice forecasts could be used (Veland et al., 2021), but dynamical sea ice prediction systems are often not able to outperform persistence of sea ice concentration (SIC) observations for short lead times (Melsom



et al., 2019; Röhrs et al., 2023; Palerme et al., 2024; Kvanum et al., 2024). Furthermore, the need for accurate sea ice forecasts is also growing due to increasing sea ice motion caused by sea ice thinning (Tandon et al., 2018; Tschudi et al., 2020).

Several studies have recently shown that data-driven sea ice forecasting systems trained on satellite observations can be skillful (e.g. Grigoryev et al., 2022; Ren et al., 2022; Chen et al., 2023; Keller et al., 2023; Koo and Rahnemounfar, 2024), and can provide more accurate forecasts than dynamical models (Andersson et al., 2021; Palerme et al., 2024; Kvanum et al., 2024). However, most operational sea ice prediction systems are still based on dynamical models (e. g. Smith et al., 2016; Barton et al., 2021; Williams et al., 2021; Ponsoni et al., 2023; Röhrs et al., 2023; Paquin et al., 2024), and there have only been a few based on machine learning approaches. The first operational data-driven sea ice prediction system developed has been IceNet (Andersson et al., 2021), which provides forecasts of the probability that SIC exceeds 15 % for the next 6 months. For lead times from 2 to 6 months, IceNet outperforms the forecasts from the European Centre for Medium-Range Weather Forecasts (ECMWF) SEAS5 seasonal prediction system (Johnson et al., 2019), while running 2000 times faster on a laptop than SEAS5 on a supercomputer. Furthermore, Palerme and Müller (2021) developed post-processed sea ice drift forecasts for lead times up to 10 days using machine learning that have been delivered on the commercial application IcySea from 2020 to 2024 (<https://driftnoise.com/icysea.html>, von Schuckmann et al., 2021).

Sea ice changes on short-time scales are primarily driven by the atmosphere, and in particular by the wind (Mohammadi-Aragh et al., 2018; Yu et al., 2020). Hence, it is crucial to include predictors from weather forecasts when developing data-driven sea ice prediction systems, as suggested by previous studies. Grigoryev et al. (2022) reported an improvement of 5 to 15 % when forecasts from the National Centers for Environmental Prediction (NCEP) operational Global Forecast System (GFS) are used, whereas Palerme et al. (2024) assessed an error reduction of 7.7 % when using ECMWF weather forecasts in addition to sea ice predictors. In this paper, we introduce MET-AICE, a data-driven sea ice prediction system producing 10-day SIC forecasts with daily time steps in the European Arctic. The predictors used in MET-AICE are derived from SIC observations provided by the Advanced Microwave Scanning Radiometer 2 (AMSR2), ECMWF weather forecasts, and a land sea mask. The forecasts have been produced daily since March 2024 and are publicly available (see code and data availability section). In section 2, the datasets used in MET-AICE and for verification are described. Then, the deep learning prediction system and the verification methods are presented in section 3. The performance of MET-AICE is evaluated and compared to the Barents-2.5km Ensemble Prediction System (EPS) in section 4, followed by the discussion and conclusions in section 5.

2 Data

2.1 Datasets used for MET-AICE

MET-AICE has been trained to predict SIC observations at about 5 km resolution derived from AMSR2 data using a three-step algorithm called reSICCI3LF (Rusin et al., 2024). The first step combines the AMSR2 microwave imagery channels at 19 and 37 GHz to derive a SIC field at about 15 km resolution with relatively low uncertainties. It then computes a higher resolution SIC field (about 5 km) using the two 89 GHz channels. This higher-resolution SIC has larger uncertainties due to the atmosphere being less transparent at these higher frequencies. Finally, the high resolution details obtained from the 89



Table 1. List of predictors used in MET-AICE.

Source	Variable	Time
AMSR2	SIC observations	Day preceding the forecast start date
AMSR2	Land sea mask	Constant predictor
ECMWF	2-meter temperature	Mean value between the forecast start date and the predicted lead time
ECMWF	10-meter x wind component	Mean value between the forecast start date and the predicted lead time
ECMWF	10-meter y wind component	Mean value between the forecast start date and the predicted lead time

55 GHz channels are added to the coarser resolution field to produce a final SIC field at 5 km resolution with relatively low uncertainties. For more details about this algorithm and product, we refer to Rusin et al. (2024) and to Palerme et al. (2024) where this product was shown to be more accurate for the ice edge position than the OSI-408-a product from the Ocean and Sea Ice Satellite Application Facility (OSI SAF), also derived from AMSR2.

The AMSR2 SIC observations from the day preceding the forecast start date are used as a predictor in MET-AICE, and
60 can be considered as the initial SIC conditions of the prediction system (table 1). The land grid points in these observations are considered as ice-free ocean (0 % SIC) since only valid values can be provided to the neural networks. MET-AICE also uses a land sea mask as a predictor, as well as ECMWF weather high-resolution forecasts (HRES, grid spacing of 9 km) in 3 predictors that are the 2-meter temperature and the 10-meter wind (x and y components on the MET-AICE grid). For the predictors from ECMWF weather forecasts, the mean values between the forecast start date and the predicted lead time are
65 used. Due to this choice, 10 different models were developed for predicting the SIC evolution during the next 10 days. All the predictors are normalized using the statistics from the training dataset (values ranging between 0 and 1), and projected onto the MET-AICE grid (Lambert azimuthal equal area at 5 km resolution) using nearest neighbor interpolation before providing them to the neural networks. In Palerme et al. (2024) and Kvanum et al. (2024), the SIC trend from passive microwave observations during the 5 days preceding the forecast start date was used as a predictor, but it was shown to have a negligible impact on the
70 predictions. Due to the limited importance of this predictor and the potential impact of missing data on the production of the forecasts, no SIC trend from satellite observations is used in MET-AICE.

2.2 Datasets used for verification

The AMSR2 SIC product from Rusin et al. (2024) is used as reference in this study since MET-AICE has been trained to predict these observations. However, passive microwave products sometimes indicate some spurious sea ice along the coasts
75 due to the difference in brightness temperatures over open water and land, as well as the spatial resolution of several kilometers (Lavergne et al., 2019; Kern et al., 2020). In order to avoid this issue, the oceanic grid points closer than 20 km from the coasts are not taken into account when the forecasts are evaluated using AMSR2 SIC observations as reference.

In addition, the ice charts produced by the ice service of the Norwegian Meteorological Institute (JCOMM Expert Team on sea ice, 2017; Copeland et al., 2024) are used as an independent dataset for verification. The ice charts, which represent sea ice



80 classes of concentration, are manually drawn by ice analysts during week days using several types of observations. Synthetic aperture radar (SAR) observations are used where they are available due to their high spatial resolution. In other areas, the analysts prioritize visible and infrared data, whereas passive microwave observations are used where no higher resolution data are available. Since the ice charts are not produced during weekends and public holidays, there are fewer data accessible for verification than using AMSR2 observations.

85 Sea ice forecasts from the Barents-2.5km EPS (Röhrs et al., 2023) are used as a benchmark in this study. Barents-2.5km EPS (hereafter referred to as "Barents-2.5") is a regional ocean-sea ice dynamical model producing hourly forecasts with lead times up to 96 hours. It consists of the Regional Ocean Modeling System (ROMS) version 3.7 (Shchepetkin and McWilliams, 2005) coupled with the Los Alamos Sea Ice Model (CICE) version 5.1 (Hunke et al., 2017). Barents-2.5 has 42 vertical layers and a spatial resolution of 2.5 km. The ensemble consists of 24 ensemble members with daily assimilation cycles (AMSR2 SIC from
90 Rusin et al. (2024), sea surface temperature, in-situ temperature and salinity observations) as well as updates of atmospheric files four times a day (six members are respectively updated at model hours 00:00, 06:00, 12:00, and 18:00 UTC). Only daily means of members produced at 00:00 UTC are used in this study for a consistent comparison with MET-AICE. In five of the six ensemble members produced at 00:00 UTC, the atmospheric forcing comes from ECMWF ensemble forecasts (ECMWF-ENS) at 9 km resolution. The remaining member is forced by the regional weather prediction system AROME-Arctic (Müller et al.,
95 2017) developed at the Norwegian Meteorological Institute, which has the same domain and spatial resolution as Barents-2.5. We chose to compare MET-AICE to Barents-2.5 since the same AMSR2 SIC observations are used to initialize both prediction systems. An ensemble Kalman filter is used to assimilate these observations in Barents-2.5, though the model's ensemble is underdispersed (lack of ensemble spread, see Idžanović et al. (2023)), which indicates an overly high confidence in the forecast and thus limits the impact of the assimilation.

100 3 Methods

3.1 Deep learning prediction system

MET-AICE is based on convolutional neural networks with a U-Net architecture (Ronneberger et al., 2015), including residual connections (He et al., 2016) and spatial attention blocks (Oktay et al., 2018). This architecture was shown to outperform the original U-Net model for short-term sea ice prediction (Palerm et al., 2024). While the residual connections are used in every
105 layer of the neural network, the spatial attention blocks are only present in the layers of the decoder. The residual connections are used to avoid vanishing issues and ease neural network training (He et al., 2016), whereas the spatial attention blocks are designed to identify and give more attention to relevant areas during training (Oktay et al., 2018). The MET-AICE grid (480 x 544 grid points) has a spatial resolution of 5 km, and the neural networks are composed of five downsampling and five upsampling operations. 32 convolutional kernels are used in the first layer, and then the number of convolutional kernels is
110 doubled at every layer in the encoder (and divided by two in the decoder). The models were trained to minimize the mean squared error during 100 epochs with a batch size of 4. An initial learning rate of 0.005 was used with an Adam optimizer,



which was then reduced by a factor of 2 every 25 epochs. In order to avoid overfitting, the model version with lowest validation loss was selected during training for each lead time. The models contain about 39 million parameters.

115 The deep learning models were trained using weekly data during the period 2013 - 2020 (about 400 forecasts for each lead time). While using weekly data decreases the size of the training dataset, this also reduces the overlap between the forecasts for long lead times, which improved the performances for lead times longer than 1 day during the tuning phase (probably due to less overfitting). Nevertheless, all the forecasts available (daily data) produced in 2021 were used for validation (for tuning the models), and all the forecasts from 2022 were used for the test dataset during the development of MET-AICE. However, this study focuses on evaluating the forecasts that have been operationally produced since March 2024. Furthermore, ECMWF
120 weather forecasts produced by different model cycles were used for training the deep learning models due to the 8-year training period (<https://www.ecmwf.int/en/forecasts/documentation-and-support/changes-ecmwf-model>).

3.2 Verification

In this study, the SIC and the ice edge position (defined by the 10 % SIC contour and excluding coastlines) are evaluated using two different verification scores. In order to assess the quality of SIC forecasts, the root mean square error (RMSE) of the SIC
125 is calculated over all oceanic grid points using AMSR2 observations as reference. Since the ice charts do not provide SIC as a continuous variable but as sea ice classes, the ice charts are only used for evaluating the ice edge position. The ice edge position is evaluated using the ratio of the Integrated Ice Edge Error (IIEE, Goessling et al., 2016) over the length of the ice edge in the observations used as reference (hereafter referred to as "ice edge distance error"). This metric was introduced by Melsom et al. (2019) and provides the mean distance between the ice edges in the forecasts and in the observations. It is worth noting
130 that normalizing the IIEE by the ice edge length (calculated using the method described in Melsom et al. (2019)) allows to use a metric which is not seasonally dependent, contrary to using the IIEE without normalization (Goessling et al., 2016; Palerme et al., 2019).

The forecasts are considered skillful if they outperform persistence of AMSR2 SIC observations from the day before the forecast start date (hereafter referred to as "persistence of AMSR2 observations"). When the ice charts are used as reference,
135 persistence of the ice charts from the day before the forecast start date (hereafter referred to as "persistence of ice charts") is used as an additional benchmark forecast, though this reduces the number of days available for verification due to the lack of ice charts during weekends and public holidays. In addition, we also developed a similar bias correction method for Barents-2.5 as the one used for TOPAZ4 in Palerme et al. (2024), where we calculate the difference between the first hourly time step from Barents-2.5 and the AMSR2 observations from the day before. Then, we subtract this difference from Barents-2.5 forecasts
140 for longer lead times in order to produce a benchmark forecast called "Barents-2.5 bias corrected" (the values lower than 0 % and higher than 100 % are then replaced by 0 % and 100 %, respectively). Due to the limitations of passive microwave SIC observations along the coasts (where spurious sea ice can be reported), this bias correction was not applied to the grid points that were closer than 20 km from the coasts. This improves the impact of the bias correction when the forecasts are evaluated using the ice charts as reference, probably due to land contamination in the passive microwave observations. The
145 bias correction used in this study is slightly different from the one proposed by Palerme et al. (2024) since the bias is calculated

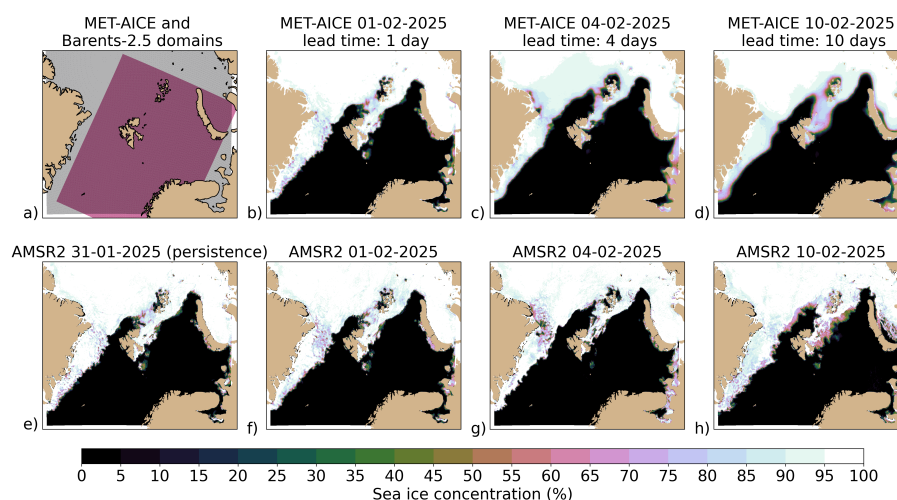


Figure 1. a) Domains of MET-AICE (gray) and Barents-2.5 (purple). Comparison between the MET-AICE forecasts initialized on the 01/02/2025 at 00:00 UTC (b to d) and the AMSR2 sea ice concentration observations for the corresponding days (f to h). e) The AMSR2 observations from the day preceding the forecast start date that are used as a predictor in the MET-AICE forecasts initialized on 01/02/2025.

using the first hourly time step from Barents-2.5 here whereas the first daily time step from TOPAZ4 was used in Palerme et al. (2024), and because the bias correction was also applied to coastal grid points in Palerme et al. (2024).

The domain of Barents-2.5 does not cover the full domain of MET-AICE (Fig.1 a). Due to the difference in model domains, the SIC forecasts are evaluated in the shared domain between Barents-2.5 and MET-AICE after projecting all the datasets on the MET-AICE grid using nearest neighbor interpolation. It is also worth noting that a common land sea mask is used for all the datasets during verification (land if there is land in at least one of the dataset).

4 Results

Fig. 1 shows the MET-AICE forecasts initialized on 01/02/2025 for lead times of 1, 5, and 10 days. During the first five days of February 2025, the surface of a polynya located around Franz Josef Land grew before closing between 05/02/2025 and 10/02/2025. MET-AICE was able to reproduce relatively well the growth and the closing of this polynya, though the magnitude of the closing was underestimated. The retreat of the ice edge north of Svalbard during the first five days of February 2025 was also predicted successfully. There was also a decrease of the sea ice extent around Novaya Zemlya which was predicted by MET-AICE, though it was slightly underestimated. However, the sea ice patches located between Svalbard and Bjørnøya remained longer than in MET-AICE predictions. Furthermore, the MET-AICE forecasts become smoother with increasing lead times, which is expected for deterministic deep learning models, as well as due to the temporal averaging of the predictors from ECMWF weather forecasts.

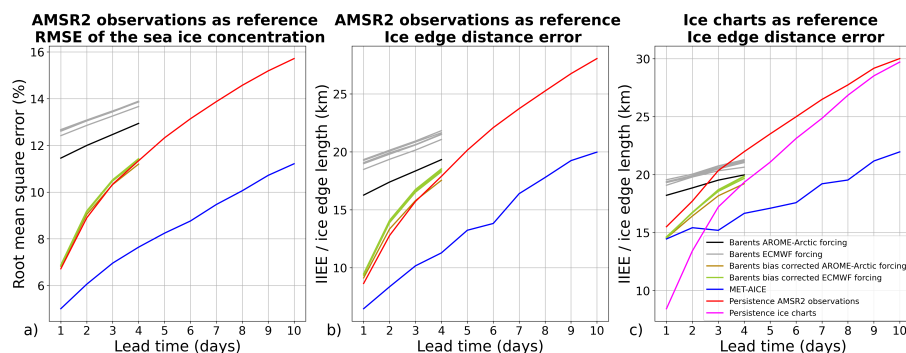


Figure 2. Performances of MET-AICE and Barents-2.5 during the period April 2024 - March 2025. a) Root mean square error (RMSE) of the sea ice concentration over the shared domain between MET-AICE and Barents-2.5 using AMSR2 observations as reference. b) Evaluation of the ice edge position (defined by the 10 % sea ice concentration contour) using AMSR2 observations as reference. c) Evaluation of the ice edge position using the ice charts as reference.

The performances of MET-AICE and Barents-2.5 for the period April 2024 - March 2025 are shown in Fig. 2. MET-AICE considerably outperforms persistence of AMSR2 observations for all lead times. When AMSR2 observations are used as reference, the RMSE of SIC for MET-AICE is about 31 % lower than for persistence of AMSR2 observations on average (between 25 % and 33 % depending on lead time). The ice edge position is also more accurate in MET-AICE, with errors about 32 % lower than for persistence of AMSR2 observations (between 25 % and 37 % depending on lead time). Barents-2.5 forecasts are less accurate than persistence of AMSR2 observations for all lead times. It is worth noting that the member forced by the regional weather prediction system AROME-Arctic outperforms the members forced by ECMWF weather forecasts, which is consistent with the findings of Idžanović et al. (2023) regarding surface currents. Nevertheless, the bias-corrected forecasts from Barents-2.5 achieve considerably better performances, comparable to persistence of AMSR2 observations.

When the ice edge position is evaluated using the ice charts as reference, MET-AICE is able to outperform persistence of AMSR2 observations for all lead times (by 24 % on average), but not persistence of the ice charts for 1-day and 2-day lead times due to the differences between the two observational products. However, MET-AICE outperforms persistence of ice charts for longer lead times, with an ice edge distance error about 8 % lower on average for all lead times. Although Barents-2.5 forecasts do not outperform persistence of ice charts for any lead time, they outperform persistence of AMSR2 observations from 3-day lead time with the member forced by AROME-Arctic, and from 4-day lead time with the members forced by ECMWF weather forecasts. Nevertheless, the Barents-2.5 bias corrected forecasts outperform persistence of AMSR2 observations for all lead times, while it is not the case when AMSR2 observations are used as reference. This is probably due to the coastal grid points (distance from the coast shorter than 20 km) which are taken into account when the ice charts are used as reference, but which are excluded when using AMSR2 observations as reference. Furthermore, the Barents-2.5 bias corrected forecasts achieve similar performances as MET-AICE for 1-day lead time, but have larger errors for longer lead times.

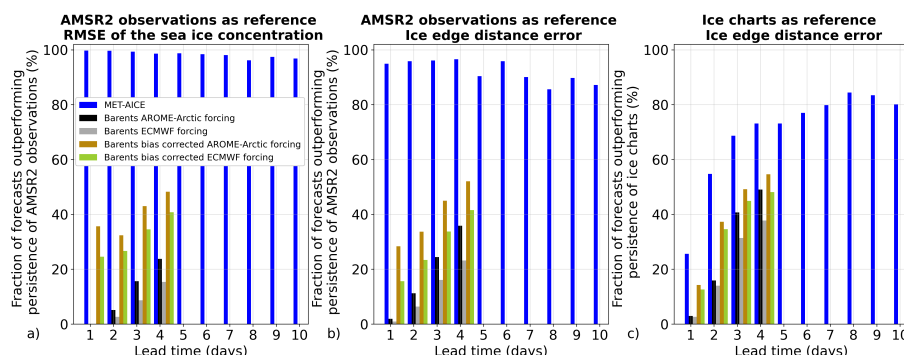


Figure 3. Fraction of days during which the forecasts outperform persistence of AMSR2 observations for the root mean square error of the sea ice concentration (a) and the ice edge position (b) using AMSR2 observations as reference during the period April 2024 - March 2025. c) Fraction of days during which the forecasts outperform persistence of the ice charts for the ice edge position using the ice charts as reference.

In Fig. 3, the fraction of days during which the forecasts can be considered skillful are shown. MET-AICE outperforms persistence of AMSR2 observations for the RMSE of the SIC between 96 % and 99.7 % of the days depending on lead time (98 % on average), and between 86 % and 97 % of the days (92 % on average) for the ice edge position using AMSR2 observations as reference. When the ice edge position is evaluated using the ice charts as reference, MET-AICE outperforms persistence of the ice charts only 26 % of the days for 1-day lead time. Nevertheless, it outperforms persistence of the ice charts 55 % of the time for 2-day lead time, and at least 68 % of the days for longer lead times. Despite the assimilation of AMSR2 SIC observations, Barents-2.5 outperforms more often persistence of the ice charts using the ice charts as reference than persistence of AMSR2 observations using AMSR2 observations as reference. This is consistent with Durán Moro et al. (2024) who also reported a better agreement between Barents-2.5 and the ice charts than with AMSR2 observations due to a higher SIC in the ice charts than in the AMSR2 product, and an over-generation of ice by the Barents-2.5 model (in particular in certain areas such as the Fram Strait).

The seasonal variability in the performances of MET-AICE and Barents-2.5 are shown in Fig. 4 and 5. When AMSR2 observations are used as reference (Fig. 4), MET-AICE considerably outperforms persistence of AMSR2 observations for all months, while Barents-2.5 has larger errors than persistence for all months. However, there is a much stronger seasonal variability when ice charts are used as reference (Fig. 5) due to the differences between the two observational products (Palerm et al., 2024). For 1-day lead time, MET-AICE never outperforms persistence of the ice charts, and has similar errors for the ice edge position as persistence of AMSR2 observations in July and August. Nevertheless, MET-AICE outperforms persistence of the ice charts most of the year for 3-day lead time, but has larger errors than persistence of the ice charts between July and September.

Fig. 6 shows the spatial variability in the performances of MET-AICE when AMSR2 observations are used as reference. It is worth noting that this figure is the result of forecasts from different seasons, and that the location of the marginal ice zone varies considerably depending on the season. In order to keep only meaningful information, the grid points with less than 50

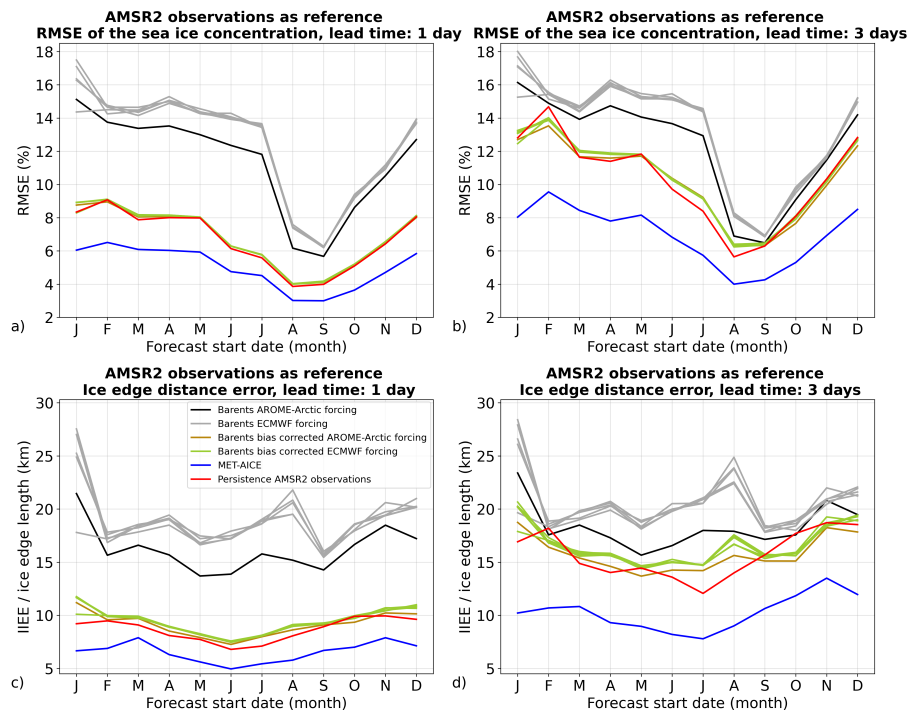


Figure 4. Seasonal variability of the performances of MET-AICE and Barents-2.5 for 1-day and 3-day lead times using AMSR2 observations as reference during the period April 2024 - March 2025. a, b) Root mean square error (RMSE) of the sea ice concentration. c, d) Evaluation of the ice edge position (defined by the 10 % sea ice concentration contour).

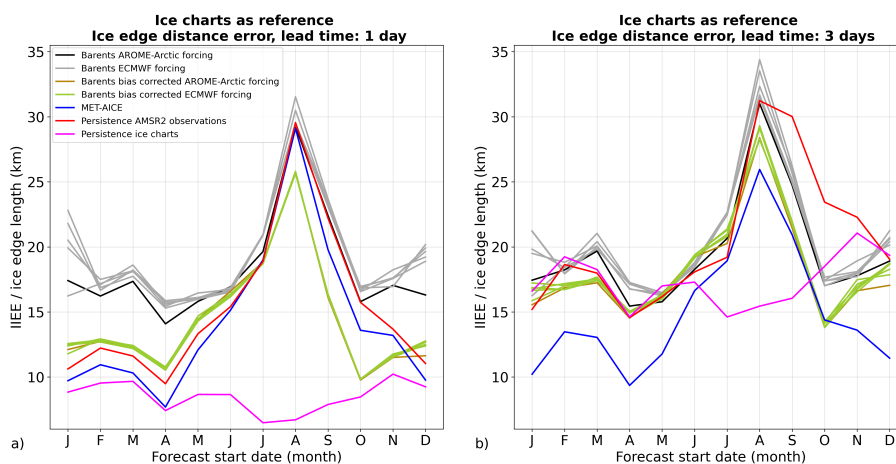


Figure 5. Seasonal variability of the performances of MET-AICE and Barents-2.5 for 1-day (a) and 3-day (b) lead times using the ice charts as reference during the period April 2024 - March 2025.

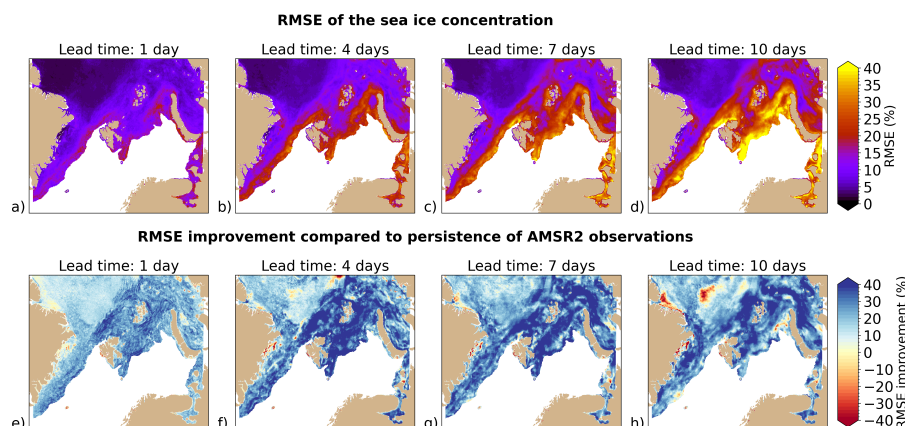


Figure 6. Spatial variability in the performances of MET-AICE using AMSR2 observations as reference. The top row shows the root mean square error (RMSE) of the sea ice concentration in MET-AICE forecasts during the period April 2024 - March 2025. The bottom row shows the relative improvement for the RMSE of the sea ice concentration of MET-AICE forecasts compared to persistence of AMSR2 observations. Positive values (blue) mean that MET-AICE outperforms persistence of AMSR2 observations. The grid points with less than 50 days during which AMSR2 observations indicate a sea ice concentration higher than 0 % are excluded from this analysis.

days during which sea ice is present (SIC higher than 0 %) are excluded from this figure. As expected, the largest errors occur where the marginal ice zone is often located, with the errors growing with increasing lead times. Furthermore, MET-AICE is able to outperform persistence of AMSR2 observations almost everywhere and for all lead times. The relative improvement compared to persistence of AMSR2 observations is larger for long lead times, in particular where the marginal ice zone is often located.

5 Discussion and conclusion

While many studies have demonstrated that data-driven sea ice forecasts can be skillful and more accurate than dynamical models (e.g. Andersson et al., 2021; Grigoryev et al., 2022; Ren et al., 2022; Chen et al., 2023; Kvanum et al., 2024), there are currently only a few of these systems running operationally. To our knowledge, MET-AICE is the first operational data-driven sea ice forecasting system focused on short and intermediate time scales (1 to 10 days). The forecasts are produced daily and are publicly available (see code and data availability section). MET-AICE is skillful for predicting AMSR2 SIC observations (that were used for training the deep learning models), and produces more accurate forecasts than the Barents-2.5 prediction system, even after bias correction. It considerably outperforms persistence of AMSR2 observations for all lead times (the RMSE of the SIC is about 31 % lower on average).

Nevertheless, passive microwave SIC observations have some limitations such as melt pond ambiguity and land contamination (Kern et al., 2016, 2020; Laverne et al., 2019). In particular, it was shown by Palerme et al. (2024) that the AMSR2 product used in MET-AICE has larger discrepancies with the ice charts close to the sea ice minimum (in August, September,



and October) compared to the rest of the year. Therefore, MET-AICE has lower skill when the ice charts are used as reference and particularly close to the sea ice minimum. We also noticed that MET-AICE sometimes predict too much sea ice along the coastlines, which is likely due to the land contamination of the passive microwave observations. It would be relevant to use other types of satellite SIC observations along the coasts in order to mitigate this issue in the future.

225 Whereas many dynamical sea ice models produce sea ice forecasts with hourly time steps (e.g. Williams et al., 2021; Ponsoni et al., 2023; Röhrs et al., 2023; Paquin et al., 2024), it is challenging to develop data-driven sea ice forecasts with such a high temporal resolution due to the limited number of observations available at this time scale. SIC and drift products with a pan-Arctic coverage are typically made available as daily averaged products (e.g. Tonboe et al., 2016; Lavergne et al., 2019; Tschudi et al., 2020; Wulf et al., 2024), limiting their usefulness for short lead times. One of the current limitations of dynamical sea
230 ice models seems to be their inaccuracy at the initial state despite using data assimilation. In the case of Barents-2.5, the large initial bias is likely due to the lack of ensemble spread, which mitigates the impact of data assimilation. A relatively simple bias correction at the initial state can greatly improve the accuracy of the forecasts as it was already shown by Palerme et al. (2024). Furthermore, this is also one of the main advantages of data-driven prediction systems which can have low biases if they are trained on a period long enough that captures the vast majority of the situations encountered.

235 The development of MET-AICE will continue in the future. It is planned to add predictions of sea ice drift and sea ice thickness since several studies have already shown the potential of machine learning for predicting these variables (e.g. Palerme and Müller, 2021; Hoffman et al., 2023; Durand et al., 2024; Koo and Rahnemoonfar, 2024; Zaatari et al., 2025). MET-AICE is currently a deterministic prediction system that was developed using the mean squared error as loss function. As a consequence, the forecasts become smoother with increasing lead times. In order to avoid this smoothing, generative artificial intelligence
240 could be used to increase the resolution of the forecasts and create a set of ensemble members. For example, Finn et al. (2024) recently showed that diffusion models can be used to produce probabilistic sea ice forecasts without reducing the effective spatial resolution.

Code and data availability. The codes used for developing and running the MET-AICE prediction system, as well as those used for the analysis are available through <https://doi.org/10.5281/zenodo.15296870> (Palerme, 2025), and in the following GitHub repository (release
245 v1.0.0): <https://github.com/cyrilpalerme/MET-AICE-v1.0/>. The MET-AICE forecasts, the AMSR2 sea ice concentration observations, and the Barents-2.5 km EPS forecasts are available on the THREDDS server of the Norwegian Meteorological Institute (https://thredds.met.no/thredds/catalog/aice_files/catalog.html, https://thredds.met.no/thredds/catalog/cosi/AMSR2_SIC/catalog.html, and https://thredds.met.no/thredds/fou-hi/barents_eps.html). A license is needed to download the operational forecasts from the European Centre for Medium-Range Weather Forecasts (ECMWF).

250 *Author contributions.* CP: conceptualization, analysis, operationalization of the forecasts, writing (original draft), and funding acquisition. JR: Operationalization of the forecasts and writing. TL: conceptualization, analysis (remote sensing), writing, and funding acquisition. JR: analysis (remote sensing) and writing. AM: writing, and funding acquisition. JB: conceptualization and writing. AFK: conceptualization and



writing. AMS: production of satellite observations. MI: operationalization of bias corrected forecasts, analysis, writing. MDM: analysis and writing. MM: writing.

255 *Competing interests.* None of the authors has any competing interests.

Acknowledgements. The development of MET-AICE was supported by the SEAFARING project funded by the Norwegian Space Agency and the Copernicus Marine Service COSI project. The Copernicus Marine Service is implemented by Mercator Ocean in the framework of a delegation agreement with the European Union. The new AMSR2 SIC observations were developed with support from the SIRANO project (Research Council of Norway; grant no. 302917).



260 References

- Andersson, T. R., Hosking, J. S., Pérez-Ortiz, M., Paige, B., Elliott, A., Russell, C., Law, S., Jones, D. C., Wilkinson, J., Phillips, T., et al.: Seasonal Arctic sea ice forecasting with probabilistic deep learning, *Nature communications*, 12, 5124, <https://doi.org/10.1038/s41467-021-25257-4>, 2021.
- Barton, N., Metzger, E. J., Reynolds, C. A., Ruston, B., Rowley, C., Smedstad, O. M., Ridout, J. A., Wallcraft, A., Frolov, S., Hogan, P.,
265 Janiga, M. A., Shriver, J. F., McLay, J., Thoppil, P., Huang, A., Crawford, W., Whitcomb, T., Bishop, C. H., Zamudio, L., and Phelps, M.: The Navy's Earth System Prediction Capability: A New Global Coupled Atmosphere-Ocean-Sea Ice Prediction System Designed for Daily to Subseasonal Forecasting, *Earth and Space Science*, 8, e2020EA001 199, <https://doi.org/10.1029/2020EA001199>, 2021.
- Chen, X., Valencia, R., Soleymani, A., and Scott, K. A.: Predicting Sea Ice Concentration With Uncertainty Quantification Using Passive Microwave and Reanalysis Data: A Case Study in Baffin Bay, *IEEE Transactions on Geoscience and Remote Sensing*, 61, 1–13,
270 <https://doi.org/10.1109/TGRS.2023.3250164>, 2023.
- Copeland, W., Wagner, P., Hughes, N., Everett, A., and Robertsen, T.: The MET Norway Ice Service: a comprehensive review of the historical and future evolution, ice chart creation, and end user interaction within METAREA XIX, *Frontiers in Marine Science*, 11, <https://doi.org/10.3389/fmars.2024.1400479>, 2024.
- Deggim, H.: The International Code for Ships Operating in Polar Waters (Polar Code), pp. 15–35, ISBN 978-3-319-78424-3,
275 https://doi.org/10.1007/978-3-319-78425-0_2, 2018.
- Durán Moro, M., Sperrevik, A. K., Laverigne, T., Bertino, L., Gusdal, Y., Iversen, S. C., and Rusin, J.: Assimilation of satellite swaths versus daily means of sea ice concentration in a regional coupled ocean–sea ice model, *The Cryosphere*, 18, 1597–1619, <https://doi.org/10.5194/tc-18-1597-2024>, 2024.
- Durand, C., Finn, T. S., Farchi, A., Bocquet, M., Boutin, G., and Ólason, E.: Data-driven surrogate modeling of high-resolution sea-ice
280 thickness in the Arctic, *The Cryosphere*, 18, 1791–1815, <https://doi.org/10.5194/tc-18-1791-2024>, 2024.
- Finn, T. S., Durand, C., Farchi, A., Bocquet, M., Rampal, P., and Carrassi, A.: Generative Diffusion for Regional Surrogate Models From Sea-Ice Simulations, *Journal of Advances in Modeling Earth Systems*, 16, e2024MS004 395, <https://doi.org/10.1029/2024MS004395>, 2024.
- Goessling, H. F., Tietsche, S., Day, J. J., Hawkins, E., and Jung, T.: Predictability of the Arctic sea ice edge, *Geophysical Research Letters*,
285 43, 1642–1650, <https://doi.org/10.1002/2015GL067232>, 2016.
- Grigoryev, T., Verezemskaya, P., Krinitskiy, M., Anikin, N., Gavrikov, A., Trofimov, I., Balabin, N., Shpilman, A., Eremchenko, A., Gulev, S., Burnaev, E., and Vanovski, V.: Data-Driven Short-Term Daily Operational Sea Ice Regional Forecasting, *Remote Sensing*, 14, <https://doi.org/10.3390/rs14225837>, 2022.
- Gunnarsson, B.: Recent ship traffic and developing shipping trends on the Northern Sea Route—Policy implications for future arctic shipping,
290 *Marine Policy*, 124, 104 369, <https://doi.org/10.1016/j.marpol.2020.104369>, 2021.
- He, K., Zhang, X., Ren, S., and Sun, J.: Deep Residual Learning for Image Recognition, in: 2016 IEEE Conference on Computer Vision and Pattern Recognition (CVPR), pp. 770–778, <https://doi.org/10.1109/CVPR.2016.90>, 2016.
- Hoffman, L., Mazloff, M. R., Gille, S. T., Giglio, D., Bitz, C. M., Heimbach, P., and Matsuyoshi, K.: Machine Learning for Daily Forecasts of Arctic Sea Ice Motion: An Attribution Assessment of Model Predictive Skill, *Artificial Intelligence for the Earth Systems*, 2, 230 004,
295 <https://doi.org/10.1175/AIES-D-23-0004.1>, 2023.



- Hunke, E., Lipscomb, W., Jones, P., Turner, A., Jeffery, N., and Elliott, S.: CICE, The Los Alamos Sea Ice Model, <https://www.osti.gov/biblio/1364126>, 2017.
- Idžanović, M., Rikardsen, E. S. U., and Röhrs, J.: Forecast uncertainty and ensemble spread in surface currents from a regional ocean model, *Frontiers in Marine Science*, 10, 1177 337, <https://doi.org/10.3389/fmars.2023.1177337>, 2023.
- 300 JCOMM Expert Team on sea ice: Sea ice information services of the world, Edition 2017, Tech. Rep. WMO-No 574, World Meteorological Organization, Geneva, Switzerland, <https://doi.org/10.25607/OBP-1325>, 2017.
- Johnson, S. J., Stockdale, T. N., Ferranti, L., Balmaseda, M. A., Molteni, F., Magnusson, L., Tietsche, S., Decremmer, D., Weisheimer, A., Balsamo, G., Keeley, S. P. E., Mogensen, K., Zuo, H., and Monge-Sanz, B. M.: SEAS5: the new ECMWF seasonal forecast system, *Geoscientific Model Development*, 12, 1087–1117, <https://doi.org/10.5194/gmd-12-1087-2019>, 2019.
- 305 Keller, M. R., Piatko, C., Clemens-Sewall, M. V., Eager, R., Foster, K., Gifford, C., Rollend, D., and Sleeman, J.: Short-Term (7 Day) Beaufort Sea Ice Extent Forecasting with Deep Learning, *Artificial Intelligence for the Earth Systems*, 2, e220 070, <https://doi.org/10.1175/AIES-D-22-0070.1>, 2023.
- Kern, S., Rösel, A., Pedersen, L. T., Ivanova, N., Saldo, R., and Tonboe, R. T.: The impact of melt ponds on summertime microwave brightness temperatures and sea-ice concentrations, *The Cryosphere*, 10, 2217–2239, <https://doi.org/10.5194/tc-10-2217-2016>, 2016.
- 310 Kern, S., Lavergne, T., Notz, D., Pedersen, L. T., and Tonboe, R.: Satellite passive microwave sea-ice concentration data set inter-comparison for Arctic summer conditions, *The Cryosphere*, 14, 2469–2493, <https://doi.org/10.5194/tc-14-2469-2020>, 2020.
- Koo, Y. and Rahnemoonfar, M.: Hierarchical Information-Sharing Convolutional Neural Network for the Prediction of Arctic Sea Ice Concentration and Velocity, *IEEE Transactions on Geoscience and Remote Sensing*, 62, 1–13, <https://doi.org/10.1109/tgrs.2024.3501094>, 2024.
- 315 Kvanum, A. F., Palermé, C., Müller, M., Rabault, J., and Hughes, N.: Developing a deep learning forecasting system for short-term and high-resolution prediction of sea ice concentration, *EGUsphere*, 2024, 1–26, <https://doi.org/10.5194/egusphere-2023-3107>, 2024.
- Lavergne, T., Sørensen, A. M., Kern, S., Tonboe, R., Notz, D., Aaboe, S., Bell, L., Dybkjær, G., Eastwood, S., Gabarro, C., Heygster, G., Killie, M. A., Brandt Kreiner, M., Lavelle, J., Saldo, R., Sandven, S., and Pedersen, L. T.: Version 2 of the EUMETSAT OSI SAF and ESA CCI sea-ice concentration climate data records, *The Cryosphere*, 13, 49–78, <https://doi.org/10.5194/tc-13-49-2019>, 2019.
- 320 Melsom, A., Palermé, C., and Müller, M.: Validation metrics for ice edge position forecasts, *Ocean Science*, 15, 615–630, <https://doi.org/10.5194/os-15-615-2019>, 2019.
- Mohammadi-Aragh, M., Goessling, H., Losch, M., Hutter, N., and Jung, T.: Predictability of Arctic sea ice on weather time scales, *Scientific reports*, 8, 6514, <https://doi.org/10.1038/s41598-018-24660-0>, 2018.
- Müller, M., Batrak, Y., Kristiansen, J., Køltzow, M. A. Ø., Noer, G., and Korosov, A.: Characteristics of a Convective-Scale Weather Forecasting System for the European Arctic, *Monthly Weather Review*, 145, 4771 – 4787, <https://doi.org/10.1175/MWR-D-17-0194.1>, 2017.
- 325 Müller, M., Knol-Kauffman, M., Jeuring, J., and Palermé, C.: Arctic shipping trends during hazardous weather and sea-ice conditions and the Polar Code's effectiveness, *npj Ocean Sustainability*, 2, <https://doi.org/10.1038/s44183-023-00021-x>, 2023.
- Oktay, O., Schlemper, J., Folgoc, L. L., Lee, M., Heinrich, M., Misawa, K., Mori, K., McDonagh, S., Hammerla, N. Y., Kainz, B., Glocker, B., and Rueckert, D.: Attention U-Net: Learning Where to Look for the Pancreas, *arXiv preprint arXiv:1804.03999*, <https://doi.org/10.48550/arXiv.1804.03999>, 2018.
- 330 Palermé, C.: Code accompanying the article "MET-AICE v1.0: an operational data-driven sea ice prediction system for the European Arctic", <https://doi.org/10.5281/zenodo.15296870>, 2025.



- Palermé, C. and Müller, M.: Calibration of sea ice drift forecasts using random forest algorithms, *The Cryosphere*, 15, 3989–4004, <https://doi.org/10.5194/tc-15-3989-2021>, 2021.
- 335 Palermé, C., Müller, M., and Melsom, A.: An Intercomparison of Verification Scores for Evaluating the Sea Ice Edge Position in Seasonal Forecasts, *Geophysical Research Letters*, 46, 4757–4763, <https://doi.org/10.1029/2019GL082482>, 2019.
- Palermé, C., Laverigne, T., Rusin, J., Melsom, A., Brajard, J., Kvanum, A. F., Macdonald Sørensen, A., Bertino, L., and Müller, M.: Improving short-term sea ice concentration forecasts using deep learning, *The Cryosphere*, 18, 2161–2176, <https://doi.org/10.5194/tc-18-2161-2024>, 2024.
- 340 Paquin, J.-P., Roy, F., Smith, G. C., MacDermid, S., Lei, J., Dupont, F., Lu, Y., Taylor, S., St-Onge-Drouin, S., Blanken, H., et al.: A new high-resolution Coastal Ice-Ocean Prediction System for the east coast of Canada, *Ocean Dynamics*, 74, 799–826, <https://doi.org/10.1007/s10236-024-01634-7>, 2024.
- Ponsoni, L., Ribergaard, M. H., Nielsen-Englyst, P., Wulf, T., Buus-Hinkler, J., Kreiner, M. B., and Rasmussen, T. A. S.: Greenlandic sea ice products with a focus on an updated operational forecast system, *Frontiers in Marine Science*, 10, 979 782, <https://doi.org/10.3389/fmars.2023.979782>, 2023.
- 345 Ren, Y., Li, X., and Zhang, W.: A Data-Driven Deep Learning Model for Weekly Sea Ice Concentration Prediction of the Pan-Arctic During the Melting Season, *IEEE Transactions on Geoscience and Remote Sensing*, 60, 1–19, <https://doi.org/10.1109/TGRS.2022.3177600>, 2022.
- Röhrs, J., Gusdal, Y., Rikardsen, E. S. U., Durán Moro, M., Brændshøj, J., Kristensen, N. M., Fritzner, S., Wang, K., Sperrevik, A. K., Idžanović, M., Laverigne, T., Debernard, J. B., and Christensen, K. H.: Barents-2.5km v2.0: an operational data-assimilative coupled ocean and sea ice ensemble prediction model for the Barents Sea and Svalbard, *Geoscientific Model Development*, 16, 5401–5426, <https://doi.org/10.5194/gmd-16-5401-2023>, 2023.
- 350 Ronneberger, O., Fischer, P., and Brox, T.: U-Net: Convolutional Networks for Biomedical Image Segmentation, *Medical Image Computing and Computer-Assisted Intervention – MICCAI 2015*, pp. 234–241, https://doi.org/10.1007/978-3-319-24574-4_28, 2015.
- Rusin, J., Laverigne, T., Doulgeris, A. P., and Scott, K. A.: Resolution enhanced sea ice concentration: a new algorithm applied to AMSR2 microwave radiometry data, *Annals of Glaciology*, p. 1–12, <https://doi.org/10.1017/aog.2024.6>, 2024.
- 355 Shchepetkin, A. F. and McWilliams, J. C.: The regional oceanic modeling system (ROMS): a split-explicit, free-surface, topography-following-coordinate oceanic model, *Ocean Modelling*, 9, 347–404, <https://doi.org/10.1016/j.ocemod.2004.08.002>, 2005.
- Smith, G. C., Roy, F., Reszka, M., Surcel Colan, D., He, Z., Deacu, D., Belanger, J.-M., Skachko, S., Liu, Y., Dupont, F., Lemieux, J.-F., Beaudoin, C., Tranchant, B., Drévilion, M., Garric, G., Testut, C.-E., Lellouche, J.-M., Pellerin, P., Ritchie, H., Lu, Y., Davidson, F., Buehner, M., Caya, A., and Lajoie, M.: Sea ice forecast verification in the Canadian Global Ice Ocean Prediction System, *Quarterly Journal of the Royal Meteorological Society*, 142, 659–671, <https://doi.org/10.1002/qj.2555>, 2016.
- 360 Stocker, A. N., Renner, A. H., and Knol-Kauffman, M.: Sea ice variability and maritime activity around Svalbard in the period 2012–2019, *Scientific Reports*, 10, 17 043, <https://doi.org/10.1038/s41598-020-74064-2>, 2020.
- Tandon, N. F., Kushner, P. J., Docquier, D., Wettstein, J. J., and Li, C.: Reassessing Sea Ice Drift and Its Relationship to Long-Term Arctic Sea Ice Loss in Coupled Climate Models, *Journal of Geophysical Research: Oceans*, 123, 4338–4359, <https://doi.org/10.1029/2017JC013697>, 2018.
- 365 Tonboe, R. T., Eastwood, S., Laverigne, T., Sørensen, A. M., Rathmann, N., Dybkjær, G., Pedersen, L. T., Høyer, J. L., and Kern, S.: The EUMETSAT sea ice concentration climate data record, *The Cryosphere*, 10, 2275–2290, <https://doi.org/10.5194/tc-10-2275-2016>, 2016.
- Tschudi, M. A., Meier, W. N., and Stewart, J. S.: An enhancement to sea ice motion and age products at the National Snow and Ice Data Center (NSIDC), *The Cryosphere*, 14, 1519–1536, <https://doi.org/10.5194/tc-14-1519-2020>, 2020.
- 370



- Veland, S., Wagner, P., Bailey, D., Everet, A., Goldstein, M., Hermann, R., Hjort-Larsen, T., Hovelsrud, G., Hughes, N., Kjøl, A., Li, X., Lynch, A., Müller, M., Olsen, J., Palerme, C., Pedersen, J., Rinaldo, Ø., Stephenson, S., and Storelvmo, T.: Knowledge needs in sea ice forecasting for navigation in Svalbard and the High Arctic, Svalbard Strategic Grant, Svalbard Science Forum. NF-rapport 4/2021, <https://doi.org/10.13140/RG.2.2.11169.33129>, 2021.
- 375 von Schuckmann, K., Le Traon, P.-Y., Smith, N., Pascual, A., Djavidnia, S., Gattuso, J.-P., Grégoire, M., Aaboe, S., Alari, V., Alexander, B. E., Alonso-Martirena, A., Aydogdu, A., J., A., Bajo, M., Barbariol, F., Batistić, M., Behrens, A., Ben Ismail, S., Benetazzo, A., Bitetto, I., Borghini, M., Bray, L., Capet, A., Carlucci, R., Chatterjee, S., Chiggiato, J., Ciliberti, S., Cipriano, G., Clementi, E., Cochrane, P., Cossarini, G., D'Andrea, L., Davison, S., Down, E., Drago, A., Druon, J., Engelhard, G., Federico, I., Garić, R., Gauci, A., Gerin, R., Geyer, G., Giesen, R., Good, S., Graham, R., Greiner, E., Gundersen, K., Hélaouët, P., Hendricks, S., Heymans, J. J., Holt, J., Hure, M.,
- 380 Juza, M., Kassis, D., Kellett, P., Knol-Kauffman, M., Kountouris, P., Kōuts, M., Lagemaa, P., Lavergne, T., Legeais, J.-F., Libralato, S., Lien, V. S., Lima, L., Lind, S., Liu, Y., Macías, D., Maljutenko, I., Mangin, A., Männik, A., Marinova, V., Martellucci, R., Masnadi, F., Mauri, E., Mayer, M., Menna, M., Meulders, C., Møgster, J. S., Monier, M., Mork, K. A., Müller, M., Nilsen, J. E. O., Notarstefano, G., Oviedo, J. L., Palerme, C., Palialexis, A., Panzeri, D., Pardo, S., Peneva, E., Pezzutto, P., Pirro, A., Platt, T., Poulain, P. M., Prieto, L., Querin, S., Rabenstein, L., Raj, R. P., Raudsepp, U., Reale, M., Renshaw, R., Ricchi, A., Ricker, R., Rikka, S., Ruiz, J.,
- 385 Russo, T., Sanchez, J., Santoleri, R., Sathyendranath, S., Scarcella, G., Schroeder, K., Sparnocchia, S., Spedicato, M. T., Stanev, E., Staneva, J., Stocker, A., Stoffelen, A., Teruzzi, A., Townhill, B., Uiboupin, R., Valcheva, N., Vandenbulcke, L., Vindenes, H., Vrgoč, N., Wakelin, S., and Zupa, W.: Copernicus Marine Service Ocean State Report, Issue 5, Journal of Operational Oceanography, 14, 1–185, <https://doi.org/10.1080/1755876X.2021.1946240>, 2021.
- Wagner, P. M., Hughes, N., Bourbonnais, P., Stroeve, J., Rabenstein, L., Bhatt, U., Little, J., Wiggins, H., and Fleming, A.: Sea-ice information and forecast needs for industry maritime stakeholders, Polar Geography, 43, 160–187, <https://doi.org/10.1080/1088937X.2020.1766592>, 2020.
- Williams, T., Korosov, A., Rampal, P., and Ólason, E.: Presentation and evaluation of the Arctic sea ice forecasting system neXtSIM-F, The Cryosphere, 15, 3207–3227, <https://doi.org/10.5194/tc-15-3207-2021>, 2021.
- Wulf, T., Buus-Hinkler, J., Singha, S., Shi, H., and Kreiner, M. B.: Pan-Arctic sea ice concentration from SAR and passive microwave, The Cryosphere, 18, 5277–5300, <https://doi.org/10.5194/tc-18-5277-2024>, 2024.
- 395 Yu, X., Rinke, A., Dorn, W., Spreen, G., Lüpkes, C., Sumata, H., and Gryanik, V. M.: Evaluation of Arctic sea ice drift and its dependency on near-surface wind and sea ice conditions in the coupled regional climate model HIRHAM–NAOSIM, The Cryosphere, 14, 1727–1746, <https://doi.org/10.5194/tc-14-1727-2020>, 2020.
- Zaatar, T., Cheaitou, A., Faury, O., and Rigot-Muller, P.: Arctic sea ice thickness prediction using machine learning: a long short-term memory model, Annals of Operations Research, pp. 1–36, <https://doi.org/10.1007/s10479-024-06457-9>, 2025.
- 400